J. Astrophys. Astr. (2000) **21**, 77-90

Stellar Sources in the ISOGAL Inner Galactic Bulge Field ($l = 0^0, b = -1^0$)

D. K. Ojha[1], A. Omont[2], S. Ganesh[3], G. Simon[4] & M. Schultheis[2],

[1] *Tata Institute of Fundamental Research, Homi Bhabha Road, Mumbai 400 005, India.*
[2] *Institut d'Astrophysique de Paris, CNRS, 98 bis, Bd Arago, F-75014, Paris, France.*
[3] *Physical Research Laboratory, Navrangpura, Ahmedabad 380 009, India.*
[4] *DASGAL, CNRS UMR 8633, Observatoire de Paris, France.*

Received 2000 March 27; accepted 2000 May 11

Abstract. ISOGAL is a survey at 7 and 15 μm with ISOCAM of the inner galactic disk and bulge of our Galaxy. The survey covers ~ 22 deg^2 in selected areas of the central $l = \pm 30$ degree of the inner Galaxy. In this paper, we report the study of a small ISOGAL field in the inner galactic bulge ($l = 0°, b = -1°$, area = 0.033deg^2). Using the multicolor near-infrared data (IJK_s) of DENIS (DEep Near Infrared Southern Sky Survey) and mid-infrared ISOGAL data, we discuss the nature of the ISOGAL sources. The various color-color and color-magnitude diagrams are discussed in the paper. While most of the detected sources are red giants (RGB tip stars), a few of them show an excess in J-K_s and K_s-[15] colors with respect to the red giant sequence. Most of them are probably AGB stars with large mass-loss rates.

Keywords. Stars: AGB and post-AGB — stars: circumstellar matter — stars: mass- loss - dust - infrared: stars — Galaxy: bulge.

1. Introduction

ISOGAL is the first detailed mid-infrared imaging survey of the inner Galaxy, tracing the Galactic structure and stellar populations. It combines 7 and 15 μm ISOCAM data with IJK_s DENIS survey available for all ISOGAL fields. The main goals of the ISOGAL survey are:

- to trace the large scale disk structure using primarily red giants (gM) old stars;
- to determine the number of (dusty) young stars;
- to map the star formation regions through diffuse ISM emission and extinction;
- to study the stellar populations and the structure of the bulge.

Multicolor mid-infrared data are essential to analyse these features. ISOGAL quantifies the distribution of the stellar populations, especially of AGB and other bright red giants, and young dusty stars mostly of intermediate mass, as well as both diffuse and dense interstellar material.

The scientific results of the analysis of the first ISOGAL field are detailed in Perault *et al.* (1996). The analysis of a small field in the inner bulge ($l = 0°$, $b = +1^0$) (Omont *et al.* 1999) confirms the importance of combining 7 and 15 μm data. It shows the remarkable capability of ISOGAL to detect and characterize

Table 1. Log of ISOCAM and DENIS observations in the l = 0.0°, b = −1.0° field.

Identification	Filter	Pixel size	Date of observations	Julian date	Remarks
13600430[b]	LW3	6″	01/04/96	24501755	12–18 μm
32500354[b]	LW2	6″	06/10/96	24503635	5.5–8.5 μm
84100927[a]	LW3	6″	05/03/98	24508785	
84100926[a]	LW2	6″	05/03/98	24508785	
DENIS[a]	I, J, K_s	1″, 3″, 3″	10/09/96	24503375	

[a]Data used in the present paper.
[b]These observations have been used for variability calculation.

mass-losing AGB and RGB tip stars. Glass *et al.* (1999) analysed the ISOGAL fields near Baade's Windows of low obscuration towards the inner parts of the bulge. Most of the detected objects towards Baade's Windows are late-type M stars, with a cut-off for those earlier than about M3-M4. The ISOGAL results are also summarized in Omont *et al.* (2000).

In this paper, we present the ISOGAL/DENIS data of a small inner bulge field (area = 0.033 deg^2), centered at $l = 0°$, $b = -1°$. We have combined the 15 μm and 7 μm ISOCAM observations with DENIS IJK_s data to determine the nature of a source and the interstellar extinction. Analysis of the sources at five near- and mid-infrared wavelengths shows that the majority of the sources are red giants with luminosities just above or close to the RGB tip. The various color-color and magnitude-color diagrams are discussed in the paper.

The outline of the paper is as follows : in section 2, we discuss the ISOGAL and DENIS observations. Section 3 describes the cross- identification of ISOGAL and DENIS sources. In section 4, we present the color-magnitude diagram of DENIS sources detected in ISOGAL. The interstellar extinction in the line of sight of the inner bulge field is described in this section. In section 5, we discuss the nature of ISOGAL sources based on multicolor near and mid- infrared data. Section 6 shows the comparison of the two inner bulge fields.

2. ISOGAL and DENIS observations

The 6″ ISOCAM* observations for the bulge field (l = 0°,b = −1°), mainly used in this paper, were performed in revolution 841 (5th March 1998) at 15 μm (filter LW3, 12 – 18 μm) and at 7 μm (filter LW2, 5.5 - 8.5 μm). We have repeated ISOGAL observations for this field with a gap of 2 years (Table 1), which were used to check the photometry, the reliability of detected sources and to identify the suspected variables in the field. A special reduction pipeline was applied to the ISOCAM data which is more sophisticated than the standard treatment and devised by Alard *et al.* (in preparation).

The histograms of the 7 and 15 μm source counts derived from the 6″ ISOGAL observations are displayed in Fig. 1. In order to ensure a reasonable level of reliability, completeness and photometric accuracy, we presently limit the discussion of ISOGAL data to sources brighter than 8.5 mag (8mJy) for LW3 sources and 9.75 mag (11 mJy) for LW2 sources (the fluxes and magnitudes used are defined in

*See Cesarsky *et al.* (1996) for a general reference to ISOCAM operation and performances. Table 1 shows the available ISOGAL and DENIS observations in detail.

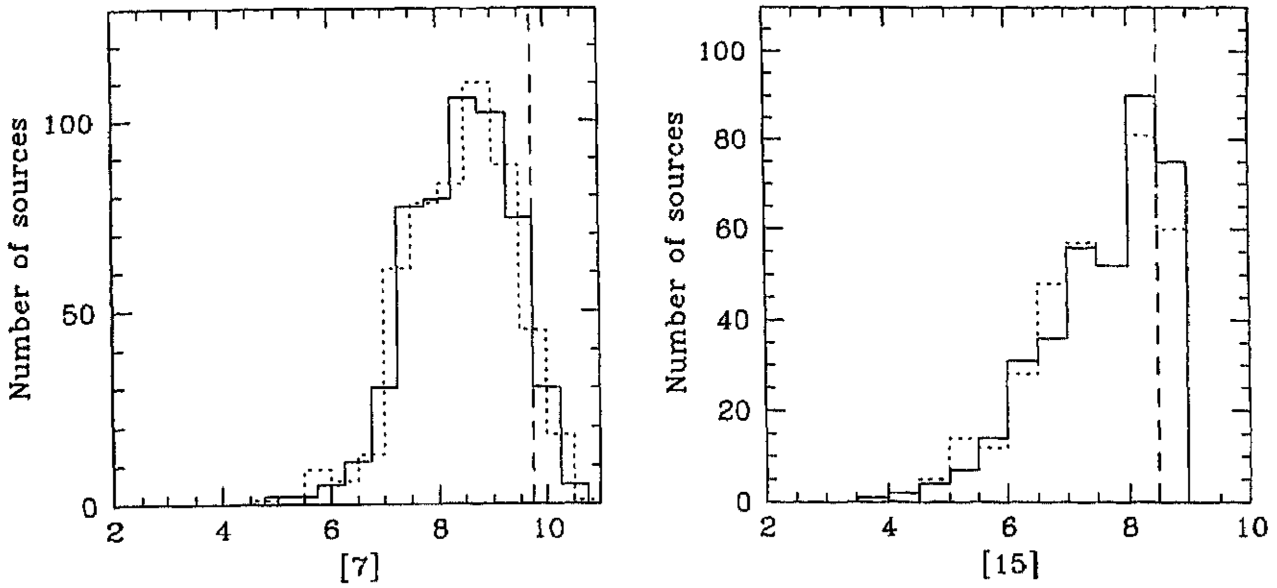

Figure 1. LW2 and LW3 source distributions in half magnitude bins. Solid lines indicate the number of detected sources in 1998 observations. Dotted lines indicate the number of detected sources in 1996 observations. Dashed lines show the limits ([7] = 9.75 and [15] = 8.5) of the sources discussed in the paper.

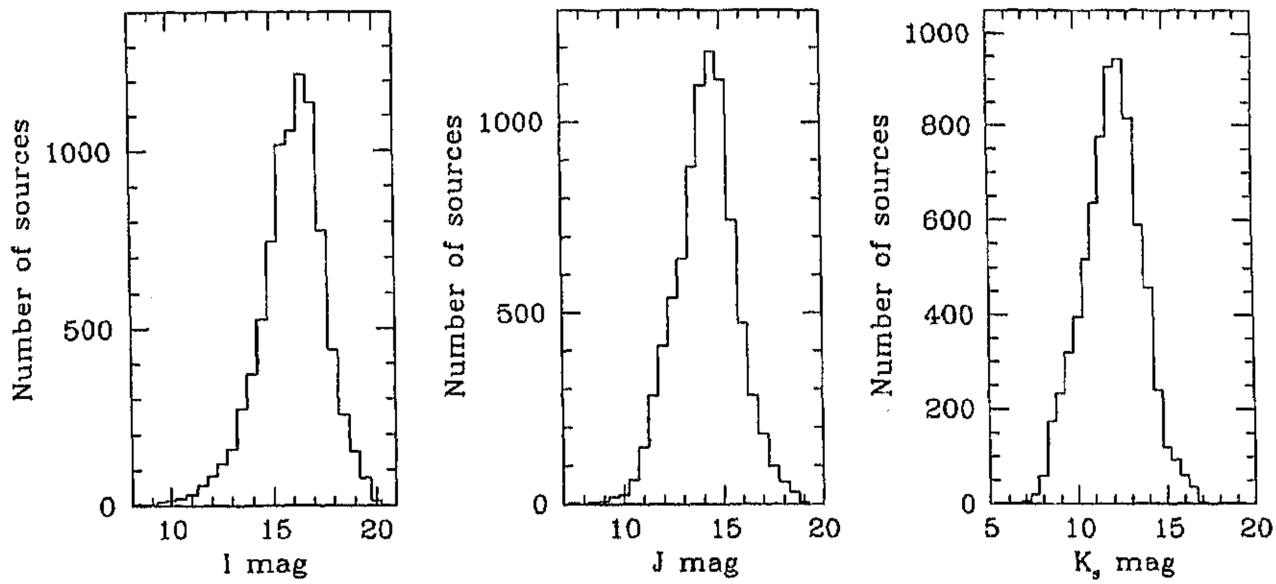

Figure 2. DENIS source counts in I, J, K_s bands in half magnitude bins.

Omont *et al.* 1999). The source counts in this field are thus 488 and 291, respectively in LW2 ([7] < 9.75) and LW3 ([15]) < 8.5). This is close to the confusion limit of 25 pixels [6″ × 6″] per source for LW2, The source densities are 1.5 10^4 deg^{-2} and 8.8 10^{-3} deg^{-2} for LW2 and LW3, respectively.

The near-infrared data used in this paper were acquired in the framework of the DENIS survey, in a dedicated observation of a large bulge field (Simon *et al.* in preparation), simultaneously in the three usual DENIS bands, Gunn-I (0.8 μm), J (1.25 μm) and K_s (2.15 μm). The region of the bulge field, which covers the ISOGAL field presented in this paper, was observed in September 1996. The histograms of the DENIS K_s, J, I sources are shown in Fig. 2. The completeness limit (due to confusion) is close to 11.5 in the K_s band and 14 in the J band.

Table 2. Catalog of bright ISOGAL + DENIS sources in the $l = 0°, b = -1°$ field ([7]) < 7.0).

No.	Name	I	J	K_s	[7]	[15]	Cross-id and comments
29	ISOGAL-DENIS-P J174906.9-293312	14.43	10.10	7.36	6.19	4.86	V
44	ISOGAL-DENIS-P J174909.1-292933	14.50	10.73	8.05	6.35	5.38	
51	ISOGAL-DENIS-P J174910.2-293441	S	S	S	6.41	6.23	F,M2 near raster edge
54	ISOGAL-DENIS-P J174910.7-293307	15.44	9.94	6.73	5.85	4.62	
87	ISOGAL-DENIS-P J174915.4-293255		11.01	7.82	6.89	5.36	
91	ISOGAL-DENIS-P J174915.9-293115	16.77	11.13	7.90	5.70	4.41	
120	ISOGAL-DENIS-P J174919.1-293325		10.49	7.53	6.39	5.40	V
132	ISOGAL-DENIS-P J174920.8-292602		10.50	7.61	5.55	4.33	
145	ISOGAL-DENIS-P J174921.8-292801		10.80	7.91	5.84	5.30	
147	ISOGAL-DENIS-P J174921.8-292523		10.95	7.82	6.92	5.95	
218	ISOGAL-DENIS-P J174926.6-293457	9.44	8.46	6.87	6.90	6.95	F,M2
314	ISOGAL-DENIS-P J174934.0-293026	15.31	10.83	8.22	6.81	5.95	
321	ISOGAL-DENIS-P J174934.4-292637	S	S	S	4.86	5.01	M4
328	ISOGAL-DENIS-P J174934.8-293041		11.35	8.66	6.98	5.37	
333	ISOGAL-DENIS-P J174935.0-292724	17.10	11.10	8.40	6.52	5.59	V
363	ISOGAL-DENIS-P J174937.1-292230		10.33	7.75	6.90	5.89	
402	ISOGAL-DENIS-P J174939.6-292722				6.66	4.64	IRAS 17464-2926
421	ISOGAL-DENIS-P J174941.2-291829			8.87	6.50	5.55	V
437	ISOGAL-DENIS-P J174942.2-292043		10.59	7.41	6.56	5.38	V
450	ISOGAL-DENIS-P J174943.3-291947		11.99	8.18	5.24	3.92	V
482	ISOGAL-DENIS-P J174946.0-292559	10.09	10.10	7.81	6.20	4.84	F,V
486	ISOGAL-DENIS-P J174946.4-292005		11.19	8.19	6.99	5.88	
488	ISOGAL-DENIS-P J174946.5-291933		10.48	7.63	6.54	5.51	
516	ISOGAL-DENIS-P J174948.8-292557	S	S	S	6.13	6.13	F
554	ISOGAL-DENIS-P J174953.8-291925	15.09	10.89	8.25	6.46	5.50	V near raster edge
562	ISOGAL-DENIS-P J174954.9-292017	13.11	9.62	7.11	6.34	5.67	V
568	ISOGAL-DENIS-P J174956.2-292530	15.27	11.32	8.53	6.68	5.56	

Note. F = Foreground star; V = Variable or suspected variable star; S = Saturated source.

3. Cross-identification of ISOGAL and DENIS sources

The cross-correlation between ISOGAL and DENIS sources has been made, which provides the multicolor data. This allows us to discuss the nature and properties of individual sources. Firstly, we have cross-correlated the ISOGAL LW2/LW3 sources. The search radius was fixed at a large value, 3.6″, for LW3/LW2 associations in order not to miss associations. The chance of spurious association with an LW2 source is then ~ 4%. Secondly, because of the very high density of DENIS sources, the search radius was reduced to 3.2″ for the DENIS/ISOGAL associations. Nevertheless, the density of the DENIS sources is so high that the chance of spurious associations remains ~ 7% for K_s sources with K_s < 10. The rms of the offsets

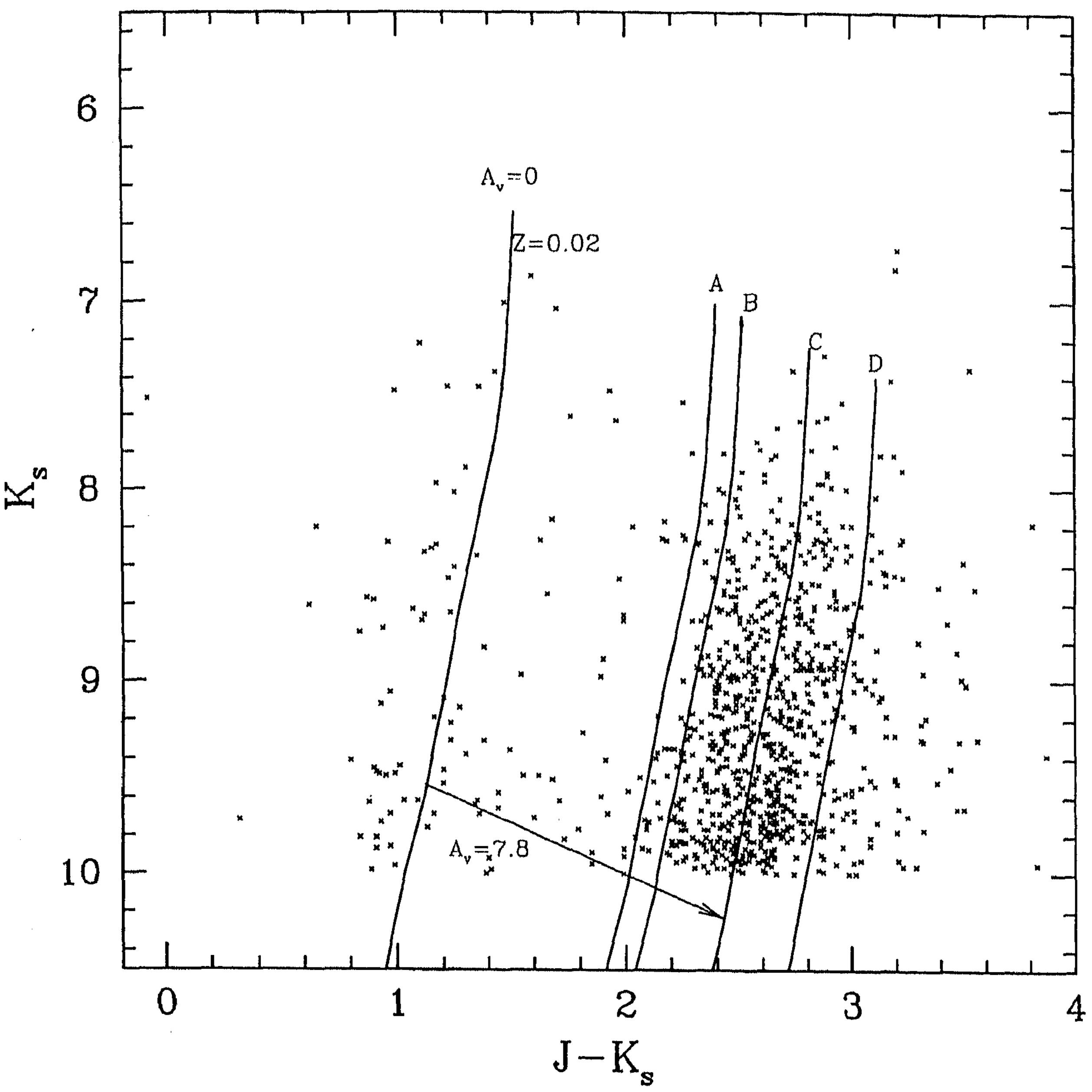

Figure 3. Color-magnitude diagram (J-K_S)/K_S for all DENIS sources in the field. An isochrone (Bertelli et al. 1994), placed at 8 kpc distance, is shown for a 10 Gyr population with Z = 0.02. The near-infrared colors of this isochrone have been computed with an empirical T_{eff} - $(J-K)_0$ color relation built by making a fit through measurements (see Schultheis et al., 1998, 1999) and Ng et al. (in preparation). The labels A, B, C, D identify the isochrones shifted by A_V of 5.3, 6.0, 7.8 and 9.6, respectively.

of matched sources are ~ 1.7″ and ~ 1.5″ for LW3/LW2 and ISOGAL/DENIS, respectively.

Thus, a substantial fraction of the ISO sources have been identified with DENIS sources. Out of a total number of 488 LW2 sources, 359 (74%) are matched with a K_s < 10 source, 353 with a JK_s source and 221 with an IJK_s source. Out of 291 LW3 sources ([15] < 8.5), 251(86%) are matched with an LW2 source, 219 (75%) with a K_s(<10)/LW2 source, 215 with a JK_s/LW2, and 133 with an IJK_s/LW2 source. The number of LW2/LW3 sources without K_s or LW3/K_s sources without LW2 is small, 32 and 24, respectively.

Table 2 gives a catalogue of bright ISOGAL sources ([7] < 7.0), with three-band DENIS associations and identification of foreground sources and of candidate

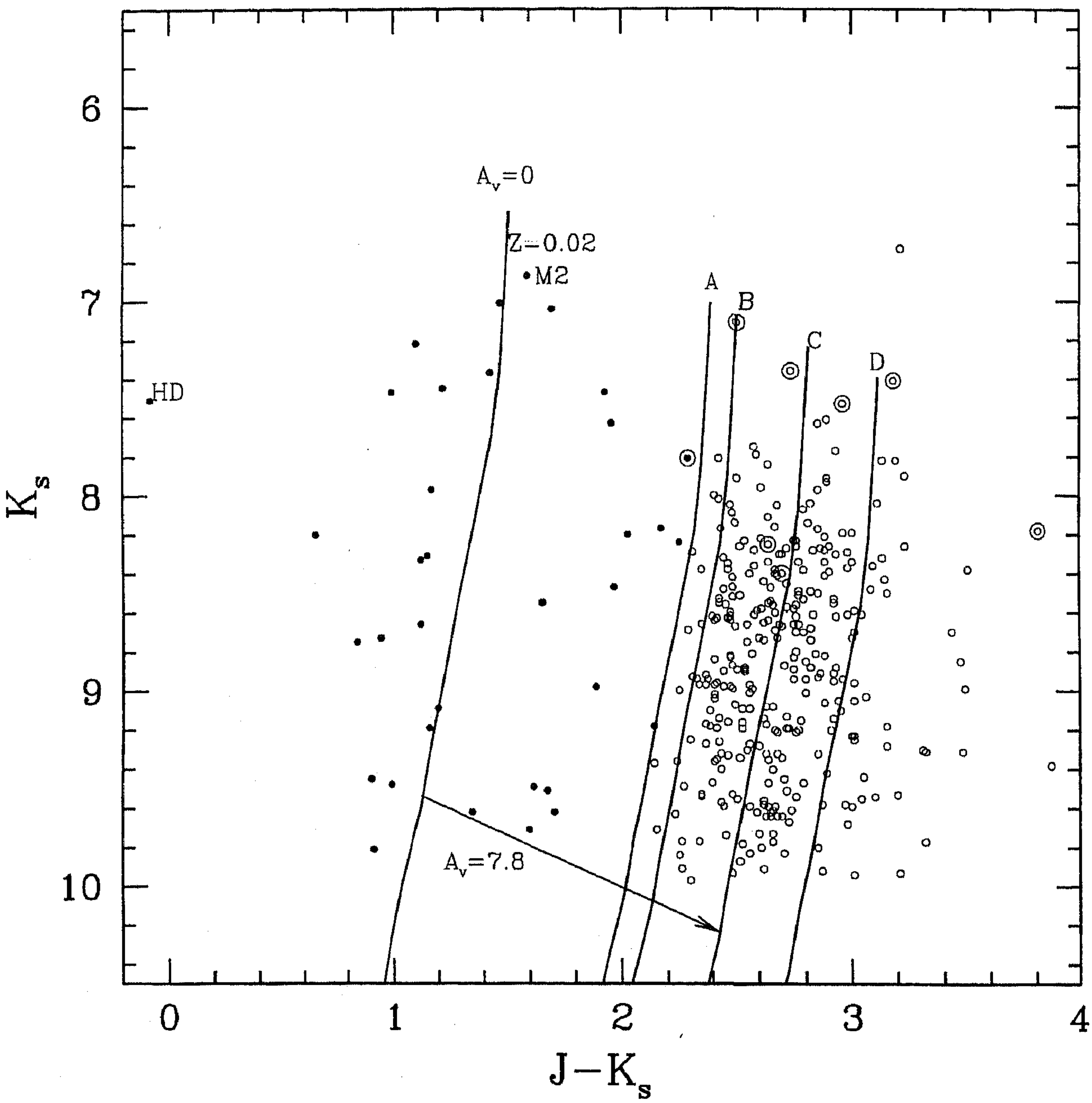

Figure 4. Color-magnitude diagram (J-K_s) /K_s for DENIS sources with [7] or [15] counterparts in the field. Filled circles represent the foreground sources with consistent data in the other diagrams. Suspected variables are indicated additionally by large open circles. The labels A, B, C, D and isochrones are as described in Fig. 3. The main sequence dwarf (HD 161908 : A9V) is denoted by HD. The M-type star in the catalog of Riharto et al. (1984) is denoted by M.

variable stars. We consider that DENIS values are saturated when $K_s < 7$, $J < 8$ and $I < 9$. The corresponding values are shown by *S* in Table 2. The cross-identified sources with SIMBAD are also shown with spectral type and IRAS name. The complete catalogue will be available at CDS, Strasbourg, within a few months.

4. Interstellar extinction

The adjunction of DENIS near-infrared data adds much to ISOGAL data, by providing different and more sensitive color indices, as well as estimates of the interstellar reddening. The K_s/J-K_s magnitude-color diagram of all DENIS sources in our field (Fig. 3) shows a bulge red giant sequence shifted and broadened by a non-uniform extinction of $A_V = 7.8 \pm 2$ magnitude with respect to the reference K_{s0} vs $(J\text{-}K_s)_0$ of Bertelli *et al.* (1994) with $Z = 0.02$ and a distance modulus of 14.5

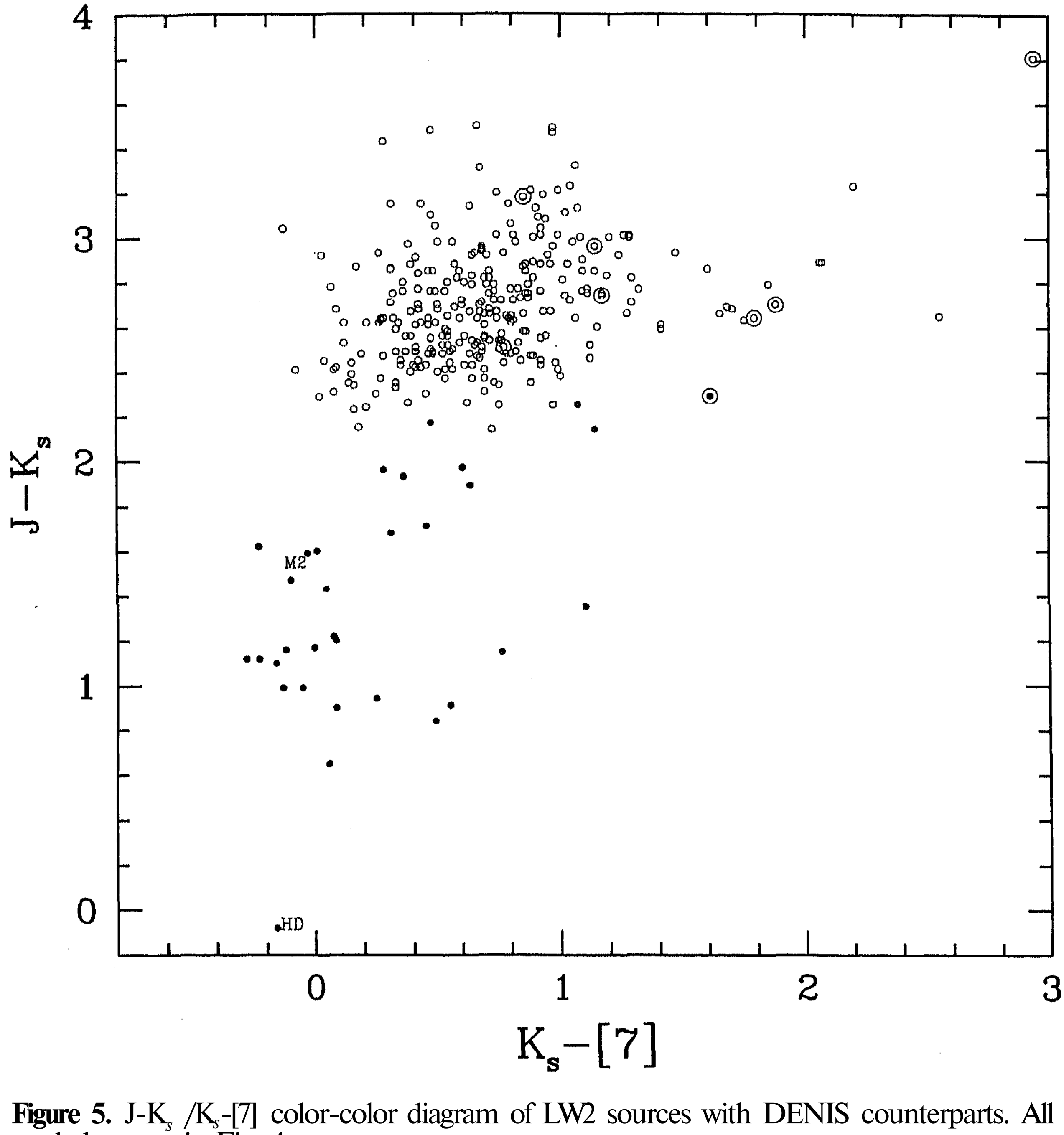

Figure 5. J-K_s /K_s-[7] color-color diagram of LW2 sources with DENIS counterparts. All symbols are as in Fig. 4.

(distance to Galactic Centre 8 kpc). We have assumed that $A_J/A_V = 0.256$; $A_{Ks}/A_V = 0.089$; $A_{[7]}/A_V = 0.027$;$A_{[15]}/A_V = 0.014$ (Glass *et al.* 1999). Most of the extinction should thus be associated with interstellar matter outside of the bulge.

The ISOGAL sources with anomalously low values of A_V are probably foreground. They are visible in Fig. 4, which shows the subset of the K_s /J-K_s sources of Fig. 3, which were also detected at longer wavelengths. The sources located left of line $A(A_V < 5.3)$ are almost certainly foreground, while those to right of line $B(A_V > 6.0)$ are very probably in the "bulge", and the case is uncertain for those between lines *A* and *B*. The J-K_s excess of the sources much redder than line D is probably most related to larger extinction rather than to exceptionally large intrinsic J-K_s excess. This is demonstrated by the values of K_s-[7] and K_s-[15], which remain characteristic of low mass-loss rates (except for the exceptional case of # 450, Table 2, there is also a group of bright stars (K_s < 8) close to line D [#54,87,91,147,137] with a moderate intrinsic J-K_s excess and a relatively strong excess at 15 μm, with the

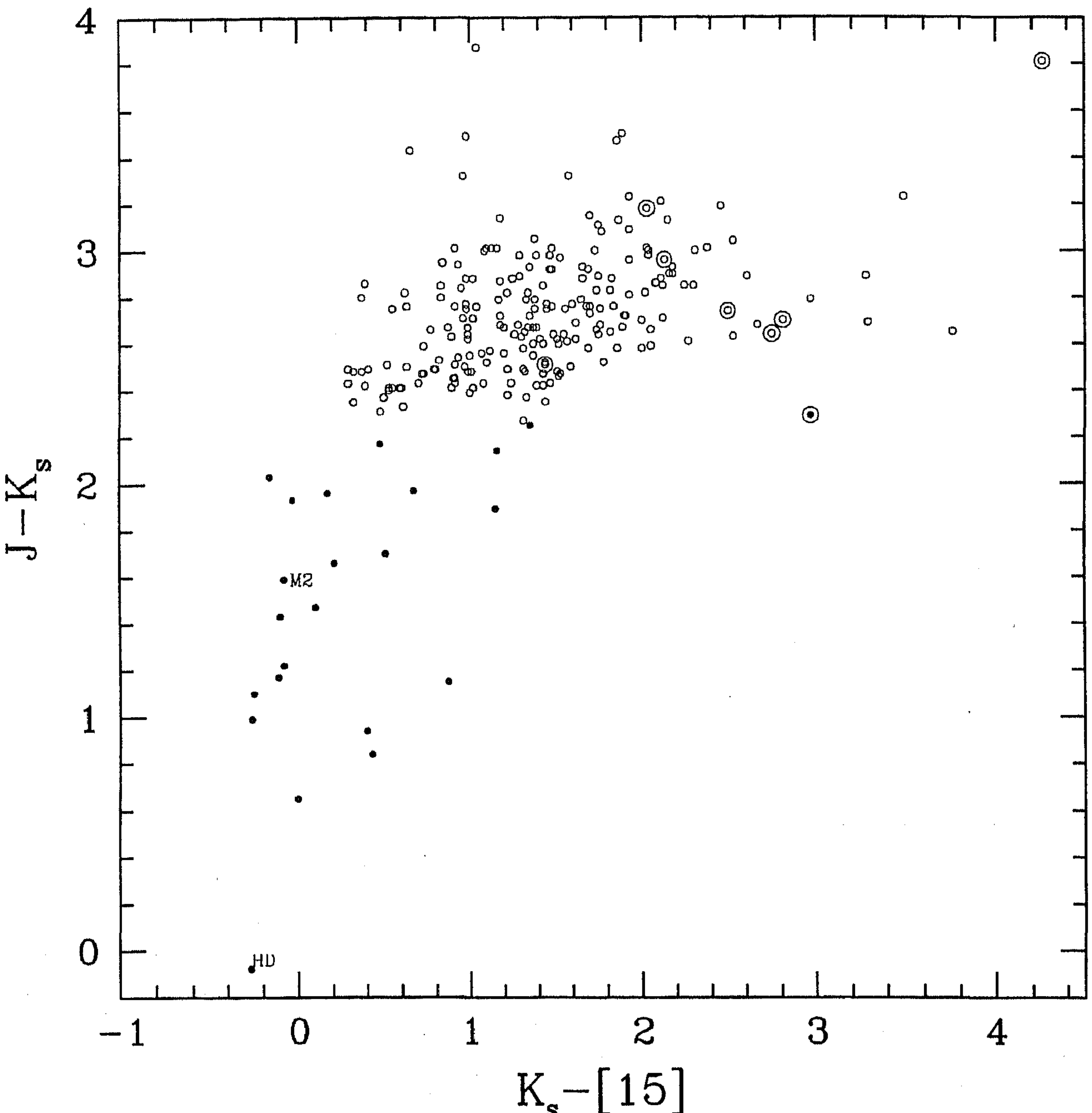

Figure 6. J-Ks/Ks -[15] color-color diagram of LW3 source with DENIS counterparts. All symbol are as in fig. 4.

characteristics of relatively large mass-loss similar to miras). Such a large extinction could correspond either to parchy dust within the bulge or to background stars.

5. The nature of the ISOGAL sources

About 35 stars (~ 10% of the ISOGAL sources with DENIS counterparts: LW2/JK$_s$), which lie to the left of the line $A(A_V$ ~ 5.3) in Fig. 4 are probably foreground stars, in front of the main line of sight extinction. About half of the foreground stars are probably red giants with practically no extinction and that their number is much larger in this field (b = — 1°) compared to the other bulge field (b = + 1°, Omont *et al.* 1999). This may be because of the dust layers which are relatively far away in b = — 1° direction. The other foreground stars with intermediate extinction look rather similar to the situation of b = +1^{0} (Omont *et al.* 1999) and are perhaps at distances comparable to that of the dust layers.

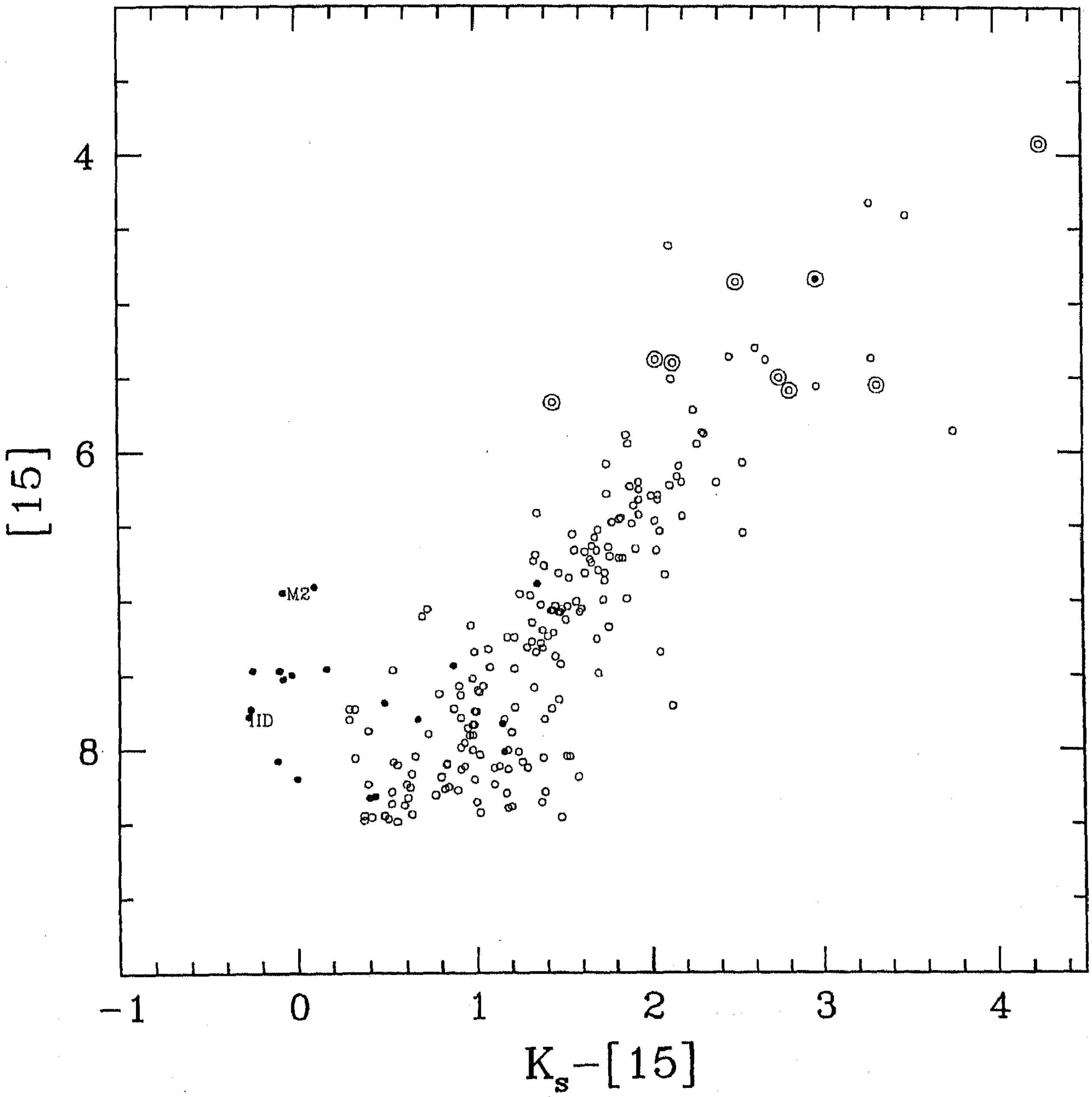

Figure 7. [15]/K$_s$-[15] magnitude-color diagram of ISOGAL sources with DENIS counterparts. Symbols are as in Fig. 4.

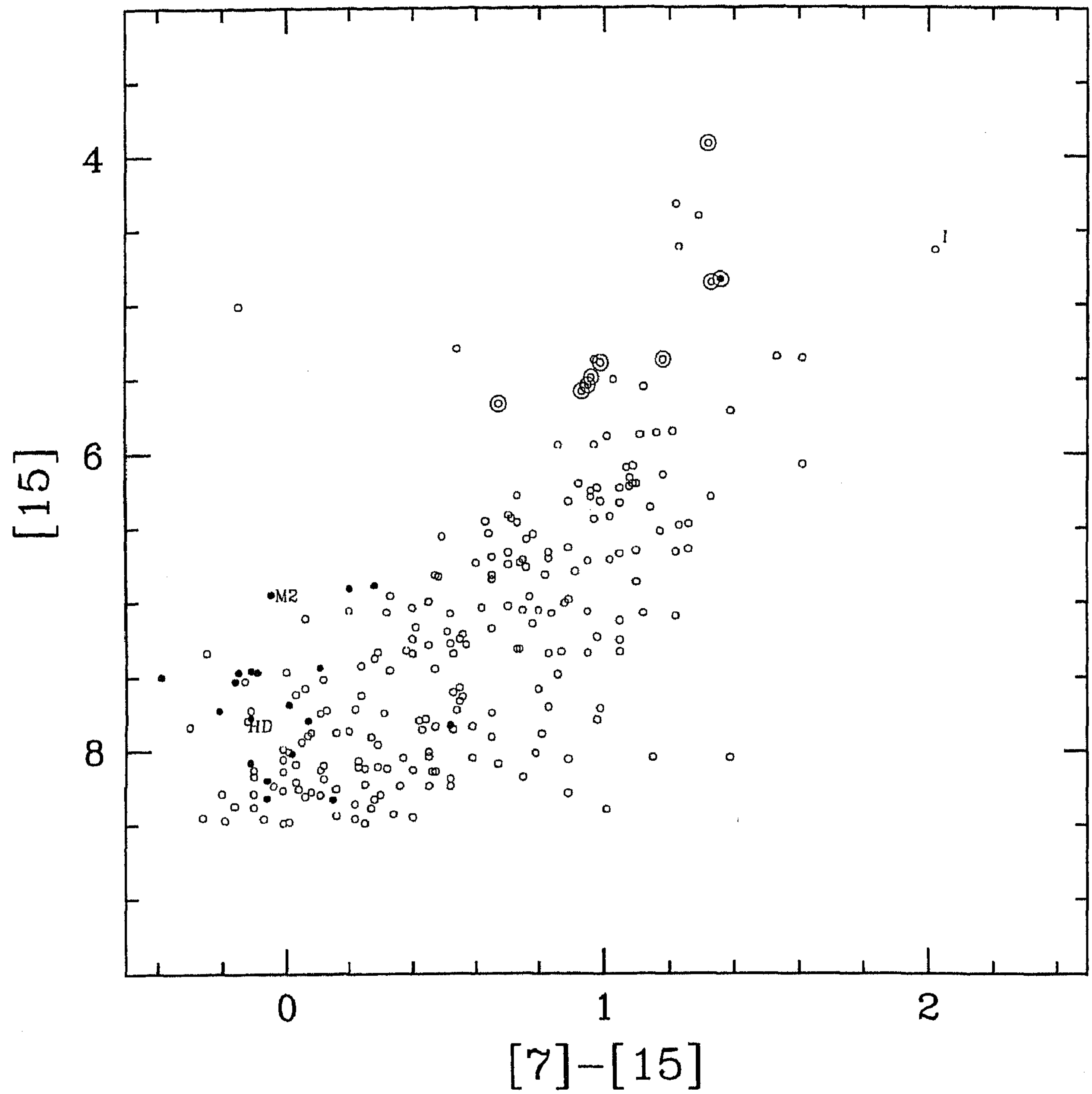

Figure 8. [15]/[7]-[15] magnitude-color diagram of ISOGAL sources. Symbols are as in Fig. 4. The IRAS source is shown by I.

The J-K_S/K_S-[7] and J-K_S/K_S-[15] color-color diagrams are shown in Figs. 5 and 6. While the range of J-K_S values is restricted to ~ 0.5 mag for most of the sources, K_S-[15] ranges from 0.3 to 2.5 for the bulk of the sources (with an extension up to 4 magnitudes for a few sources). The colors [7]—[15] and K_S-[7] (Figs. 8 and 10) also display large ranges of excess, although somewhat smaller than for K_S-[15]. More than half of the sources under discussion have observed K_S-[15] colors redder than ~ 1, and very red [7]—[15] colors. Only the presence of the circumstellar dust can explain such a large excess. These data suggest that these are intermediate AGB stars or RGB tip stars with low and high mass-loss rates as discussed below.

The magnitude-color diagrams [15]/K_S-[15] and [15]/[7]—[15] are shown in Figs. 7 and 8, respectively. Characteristic values of the colors and magnitudes corresponding to the two ends of the intermediate AGB sequence are given in Table 3. The magnitude of the lower end of the sequence coincides with the ISOGAL sensitivity at 15 μm, which is almost exactly that of the tip of the bulge RGB (K_0 ~ 8.2,

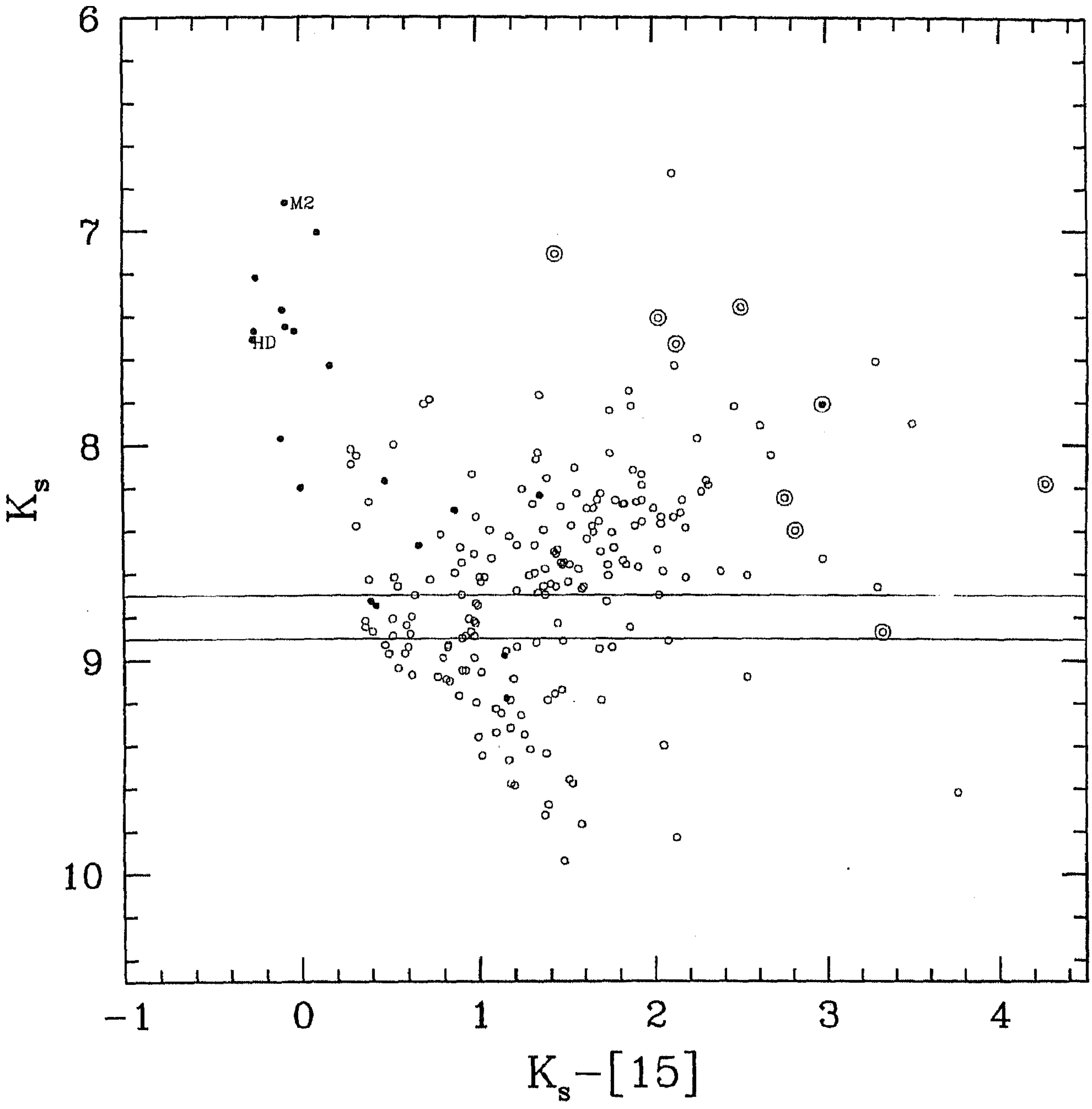

Figure 9. K_s/K_s-[15] magnitude-color diagram of ISOGAL sources detected both in LW2 and LW3, with DENIS counterparts. The approximate position of the RGB tip (taking into account the interstellar extinction in this field) is shown by the solid lines at $K_s = 8.9$ ($K_0 \sim 8.2$, Tiede *et al.* 1996) and $K_s = 8.7$($K_0 \sim 8.0$, Frogel *et al.* 1999). All symbols are as in Fig. 4.

Tiede *et al.* 1996; $K_0 \sim 8.0$, Frogel *et al.* 1999). This K_{s0} magnitude range, 7.6 - 8.3 (Table 3), corresponds to M spectral types from M6 to M9 (Frogel & Whitford 1987 & Glass *et al.* 1999). This sequence of stars is described as "intermediate-AGB mass-loss sequence" (Omont *et al.* 1999).

From the SIMBAD data base, we have identified five sources in this field. [RHI84] 10-714 (M2), [RHI84] 10-733 (M2) and [RHI84] 10-745 (M4) are M-type stars in the catalogue by Riharto *et al.* (1984). These sources are denoted by "M" in Fig. 4. HD 161908 is an early main-sequence star with spectral type A9V. It is denoted by "A" in the figures. IRAS 17464-2926 with $S_{25\,\mu m}S_{12\,\mu m}$ = 0.77 and [7]-[15]= 2.13 is denoted by " I " in Fig. 8.

In order to investigate the variability in this field, we have compared the repeated observations performed with 6″ pixels, at two different dates (a gap of 2 years) with

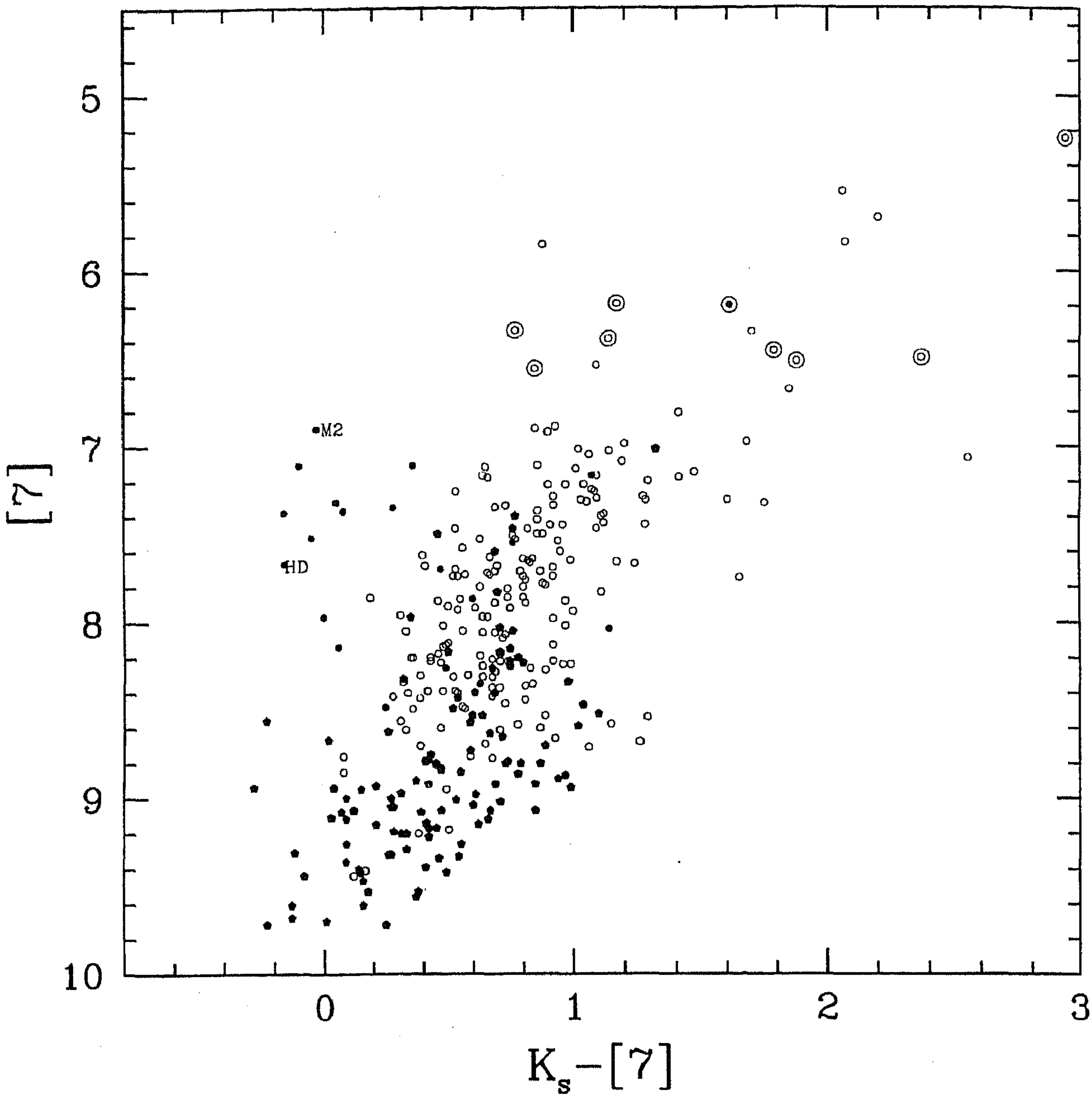

Figure 10. [7]/K_s-[7] magnitude-color diagram of all LW3 sources with DENIS counterparts. Filled asterisks represent sources without a detection at LW3. All other symbols are as in Fig. 4.

Table 3. Values of colors and magnitudes for the base and the tip of the mass-loss AGB sequence in the magnitude-colors diagrams in Figs. 7, 8 and 9.

	K_s–[15]	[7]–[15]	[15]	K_s	$(K_s - [15])_0$	K_{s0}	$M_K^{(a)}$	$M_{\rm bol}^{(b)}$	$L(L_\odot)$
Tip	2.3	1.3	6.0	8.3	1.7	7.6	−6.9	−3.9	2884
Base	0.5	0.0	8.5	9.0	−0.1	8.3	−6.2	−3.2	1514

[(a)] With a distance modulus of 14.5 (D = 8 kpc).

[(b)] With the K bolometric correction $M_{\rm bol} - M_{K_S} = 3.0$ (Groenewegen 1997), which yields $M_{\rm bol} \sim K_s - 12.2$ in this field.

both LW2 and LW3 filters (Table 1). Only a bright source has been considered for the variability, where there is a 3σ difference in one band. The sources selected in this way are displayed with special symbols in various figures. The repeated DENIS observations will also be used to look for the variable stars in all the inner bulge fields (Schultheis *et al.,* in preparation).

6. Comparison with bulge ($l = 0°, b = +1°$) field

We have compared the results of the bulge field (present paper) with another ISOGAL bulge field at $l = 0°, b = +1°$, area = 0.033 deg^2. This field was analysed in detail and the results published in the paper by Omont *et al.* (1999). 3″ ISOCAM observations are mainly used in this paper. However, the same field was also observed with ISOCAM in revolution 836 with 6″ pixel size at LW3 and LW2, respectively (see Table 1 by Omont et al. 1999). To make a direct comparison between the two ($b = -1°$ & $b = +1°$) inner bulge fields, we have also analysed the 6″ data of $b = +1°$ field. A detailed evaluation of 6″ ISOCAM data of a few inner bulge fields including the $b = +1°$ will be presented elsewhere (Ojha *et al.,* in preparation).

The bulge field at $b = -1°$ seems to suffer more extinction (by ~ 2 magnitudes) and is more patchy compared to $b = +1°$ field. The source density in both LW2 and LW3 filters is higher (by a factor of ~ 1.2) in $b = -1°$ than in $b = +1°$ field. The density of foreground stars is larger in $b = -1°$ field by a factor of 1.5 compared to $b = +1°$ field. The density of foreground ISOGAL sources with DENIS JK_s counterparts is 1061 per deg^2 in $b = -1°$ field, while it is 697 per deg^2 in $b = +1°$ field. The origin of such differences is not entirely clear.

7. Conclusion

We have shown that the combination of near-infrared (DENIS) and mid-infrared (7 and 15 μm ISOGAL data allows reliable detection AGB and RGB tip stars. We conclude that most of the ISOGAL sources detected both at 7 and 15 μm in the inner bulge field are intermediate AGB stars or RGB tip stars with low and high mass-loss rates. The sequence in various color-magnitude diagrams is well coincident with the late M AGB sequence, from M6 to M9, just above the RGB tip.

Acknowledgements

This publication makes use of data based on observations with ISO, an ESA project with instruments funded by ESA Member States (especially the PI countries: France, Germany, the Netherlands and the United Kingdom) and with the participation of ISAS and NASA. DENIS data are based on observations collected at the European Southern Observatory, La Silla, Chile. The DENIS project is partially funded by European Commission through SCIENCE and Human Capital and Mobility plan grants. It is also supported, in France by the Institut National des Sciences de 1'Univers; the Education Ministry and the Centre National de la Recherche Scientifique; in Germany by the State of Baden-Würtemberg; in Spain by the DG1CYT; in Italy by the Consiglio Nazionale delle Ricerche; in Austria by the Fonds zur Förderung der wissenschaftlichen Forschung und Bundesministerium für Wissenshaft und Forschung; in Brazil by the Foundation for the development of Scientific Research of the State of Sao Paulo (FAPESP); and in Hungary by an OTKA grant and an ESOC&EE grant. This research has made use of the DEC-ALPHA system of the Optical CCD astronomy programme of TIFR.

References

Bertelli, G., Bressan, A., Chiosi, C., Fagotto, F., Nasi, E. 1994, *Astr. Astrophys,* **106,** 275.

Cesarsky, C. *et al.* 1996, *Astr. Astrophys,* **315L,** 32.

Frogel, J. A., Whitford, A. E. 1987, *Astrophys J.,* **320,** 199.

Frogel, J. A., Tiede, G. P., Kuchinski, L. E. 1999, *Astrophys J.,* **117,** 2296.

Glass, I. S., Ganesh, S., Alard, C., Blommaert, J. A. D. L., Gilmore, G., Lloyd Evans, T., Omont, A., Schultheis, S., Simon, G. 1999, *Mon. Not. R. astr. Soc.,* **308,** 127.

Groenewegen, M.A.T. 1997, in *The Impact of Large Scale Near-IR Sky Surveys,* (eds). F. Garzon *et al* (Kluwer) page 165.

Omont, A., Ganesh, S., Alard, C, Blommaert, J. A. D. L., Caillaud, B., Copet, E., Fouqué P., Gilmore, G., Ojha, D. *et al.* 1999, *Astr. Astrophys,* **348,** 755.

Omont, A. and The ISOGAL Collaboration 2000, In Springer Lecture Notes of Physics Series, as part of the proceeding for "ISO Surveys of a Dusty Universe", a workshop held at Ringberg Castle, Germany, November 8-12, 1999.

Pérault, M., Omont, A., Simon, G., Séguin, P., Ojha, D. *et al.* 1996, *Astr. Astrophys,* **315,** L165.

Riharto, M., Hamajima, K., Ichikawa, T., Ishida, K., Hidayat, B 1984, *Ann. Tokyo Astron. Obs.,* 2nd Series, Vol. 19, No. 4, page 469.

Schultheis, M., Ng, Y. K., Hron, J., Kerschbaum, F. 1998, *Astr. Astrophys,* **338,** 581.

Schultheis, M., Ganesh, S., Simon, G., Omont, A., Alard, C., Borsenberger, J., Copet, E., Epchtein, N., Fouqué, P. Habing, H. 1999, *Astr. Astrophys,* **349,** L69.

Tiede, G.P., Frogel, J.A., Terndrup, D.M. 1996, *Astr. J.,* **110,** 2788.